Vol 13 No 3, March 2004
1009-1963/2004/13(03)/0359-05

Chinese Physics

© 2004 Chin. Phys. Soc.
and IOP Publishing Ltd

Optical breakdown and filamentation of femtosecond laser pulses propagating in air at a kHz repetition rate*

Duan Zuo-Liang(段作梁)†, Chen Jian-Ping(陈建平), Li Ru-Xin(李儒新), Lin Li-Huang(林礼煌), and Xu Zhi-Zhan(徐至展)

Laboratory for High Intensity Optics, Shanghai Institute of Optics and Fine Mechanics, Chinese Academy of Sciences, Shanghai 201800, *China*

(Received 17 January 2003; revised manuscript received 8 May 2003)

We report the experiments on the optical breakdown and filamentation of femtosecond laser pulses propagating in air at a kHz repetition rate and with several hundreds micro-joule-energy. A 10m-long filament and its breakup and merging at the nonlinear focal region produced by modulational instability of femtosecond laser pulses in air are observed. A simple model based on the nonlinear Schrödinger equation coupled with multiphoton ionization law is presented to explain the several experimental results.

Keywords: filamentation, Kerr self-focusing, optical-breakdown
PACC: 4265J, 5235M

1. Introduction

In recent years, there has been an interest in the filamentation of powerful femtosecond laser pulses resulting from their propagation over long distances in air.[1−8] A filament can persist a long distance from over tens of metres in air and up to several kilometres in atmosphere. Its main physical mechanism is the dynamic balance between Kerr self-focusing of the nonlinear effects of the intense laser beam propagating in air and defocusing of the plasma generated by laser-induced ionization of oxygen and nitrogen in air and diffraction of the laser beam. Other effects such as group velocity dispersion, multiphoton absorption, absorption loss of the plasma and refraction of the plasma should be included. The filaments typically have the energy of several tenths of millijoule, a diameter ranging from 40μm to several millimetres and a red-shifted spectrum.[1]

The detailed characteristics of the filament such as white-light supercontinuum generation, the clamping of power in the filament, multifilament, spectra broadening, and high-order harmonic generation have been studied by Aköbek's group.[9] The applications of the phenomena in filaments include remote sensing [10] and lightning discharge control.[11−13]

In this paper, we report here some new results on the characterization of filamentation of femtosecond laser pulses. The energy of the filamentation is significantly lower ($\sim$ 0.7mJ) than that elsewhere.[3−5] We have observed the filament formed over 10m. A lens (f=14m) is used to converge the laser beams. Before the focus of the lens two filaments can be observed, but they become a single filament behind the focus of the lens. A simple model based on nonlinear the Schrödinger(NLS) equation coupling to multiphoton ionization law is proposed to explain the several experimental results. Finally, we use a variational method to analyse the equation of femtosecond laser pulses propagatiing in air. It allows us to obtain an easy semianalytical solution to the problem.

2.Experiment and model

2.1. Experiment

In our experiments, femtosecond laser pulses are

*Project supported by the National Natural Science Foundation of China (Grant No 29890210), the National Basic Research Special Foundation (Grant No G1999075200) and Shanghai Foundation of Science & Technology (Grant No 0159nm022).
†E-mail: duanzl_213@mail.siom.ac.cn

produced by a Ti:sapphire laser system at a 1kHz repetition rate, central wavelength of 795nm, pulse energy of about 0.7mJ, pulse duration of 50fs, with diameter of laser beam $a = 7.0 \pm 0.3$mm ($1/e^2$ level of intensity) and the beam quality $M^2 < 1.3$. The temporal profile of laser pulse was measured using a single-shot, second-order autocorrelator. The laser beam is converged by a lens to make the beam shrink. We define the central plane of the lens as the origin of the propagation axis in air. The energy of the femtosecond laser pulse is adjusted between 0.2 and 0.7mJ for different conditions with $\lambda/2$ wave plate and a polarizer, corresponding to peak power values ranging from about 4 to 14GW for the 50fs pulses. This power is several times the theoretical value of the critical power $P_{\rm cr}$ for the onset of filamentation:

$$P_{\rm cr} = \frac{\lambda_0^2}{2\pi n_0 n_2}, \tag{1}$$

where λ_0 is the central wavelength of femtosecond laser pulse, n_0 is the linear refraction index of the air, n_2 is the nonlinear refraction index of the air, $n_2 = 12\pi^2\chi^{(3)}/(n_0^2 c) \approx 5.0 \times 10^{-19}{\rm cm}^2/{\rm W}$.

In our experiments, we used lenses with different focal lengths (f=5cm, 10cm, 20cm, 100cm, 200cm, 400cm, 800cm, 1000cm, and 1400cm) to converge the laser beams. We observed that the shorter the focal length, the brighter the spark of nonlinear focal length ($< f$) is. The actions of the convergence by the lens with a short focal length and Kerr self-focusing of nonlinearity of the air converge the laser beams and produce high electronic density that diverge the laser beams strongly. So the long filament cannot form. The white-light continuum generation resulting from the self-steepening terms of the powerful femtosecond laser pulse propagating in the air causes strong blue shifting of the spectrum.[14,15]

When the focal length of the lenses increases from 5 to 1400cm, the spark diminishes and even vanishes. The filament of plasma appears and becomes longer with the increase of the lens focal length. For the filament produced with the lens with f=14m, there are two filaments at the beginning of filamentation, and the two filaments merge into one gradually along the direction of propagating axis. Tzortzak[16] has pointed out that the breakup and the merging of the filament are formed by the modulational instability of the femtosecond laser pulses propagating in air. We find, however, the aberration of the lens could play a role in the process of the breakup and the merging of the filament, such as that two sparks in sequence appear when the laser beam is not perpendicular to the plane of the lens. This phenomenon cannot be observed in the filament process of collimating a femtosecond laser pulse propagating in the air.

For laser intensity less than $10^{13}{\rm W/cm}^2$ (i.e. outside the filament region), the beam splitter (BS) and the pickup plate surfaces are not optically damaged, so the reflected part of the laser beam is not distorted. We have obtained the intensity distribution of laser pulses in the transverse plane, and used the BS to pick up the laser beam. The reflected part of the laser beam is imaged with a large numerical aperture lens onto a CCD camera. The intensity profiles of the self-channelling pulse are measured along the propagation axis. The diameter of the filament is recorded with a large numerical aperture lens imaging onto a CCD camera after being scattered off by a scattering plate at an angle of 45°.

2.2. Model of the laser beam propagation

We consider the propagation of the linearly polarized laser beam in the air. From Maxwell's equations we start from the following scalar wave equation:

$$\frac{\partial^2 E}{\partial x^2} + \frac{\partial^2 E}{\partial y^2} + \frac{\partial^2 E}{\partial z^2} - \frac{\varepsilon_0}{c^2}\frac{\partial^2 E}{\partial t^2} - \triangle n_r E = 0, \tag{2}$$

where $\triangle n_r$ is the varying part of the nonlinear refraction index of the air under the powerful light intensity, and ε_0 is the linear dielectric constant of air. The electric field can be written as

$$E(x,y,z,t) = A(x,y,z,t)\exp[-{\rm i}(wt - kz)] + {\rm c.c.}, \tag{3}$$

where $A(x,y,z,t)$ is assumed to be a slowly varying amplitude of the electric field, k is the linear wavenumber. Substituting Eq.(3) in Eq.(2), applying the slowly envelope approximation, and in the frame of reference of the retarded time coordinate $\tau = t - z/v_{\rm g}$ where $v_{\rm g}$ is the group velocity of light in the air, we obtain the well-known NLS equation

$${\rm i}\frac{\partial A}{\partial z} + \frac{1}{2k}\left(\frac{\partial^2 A}{\partial x^2} + \frac{\partial^2 A}{\partial y^2}\right) + k\delta n A + {\rm i}\gamma A = 0 \tag{4}$$

and

$$\delta n = n_2 I - \frac{n_{\rm e}}{2n_{\rm c}}, \tag{5}$$

where n_2 is the nonlinear refraction index of air, $n_{\rm e}$ is the electron density of plasma, $n_{\rm c} = m_{\rm e}\omega^2/(4\pi {\rm e}^2)$ is the plasma critical density, iγ denotes the attenuation of the pulse. We consider that multiphoton absorption is the main factor causing attenuation of the

laser pulses, so $\gamma = K\hbar\omega n_0\beta^{(K)}I^{K-1}/2$. The electron density n_e is governed by

$$\frac{\partial n_e}{\partial \tau} = N_0 R(|A|^2), \tag{6}$$

where $N_0 = 2.7 \times 10^{19}/\mathrm{cm}^3$ is the density of neutral atoms, and $R(|A|^2) = \beta^{(K)}|A|^{2K}$ is the rate of ionization for oxygen (nitrogen), K is the effective order of the ionization process, for oxygen $\beta^{(K)} = 1.29\times10^{-65}\mathrm{cm}^{2K}\mathrm{W}^{-K}\mathrm{s}^{-1}$ with K=5.51 and for nitrogen $\beta^{(K)}$=$4.45\times10^{-84}\mathrm{cm}^{2K}\mathrm{W}^{-K}\mathrm{s}^{-1}$ with K=6.78.[17] Equation (6) can be integrated to yield

$$n_e = \int_{-\infty}^{\tau} N_0\beta^{(K)}|A|^{2K}\mathrm{d}\tau'. \tag{7}$$

Since A is a slowly varying envelope function, the electron density can be approximated to an integral to the peak of the pulse,[10] $n_e = g(\tau)N_0\beta^{(K)}|A|^{2K}$, $g(\tau) = (\tau_{\min}+\tau)/2$ and $\tau_{\min}$ is a cutoff determined by the initial pulse.

We use a variational method to solve the above NLS equation.[18,19] Here we assume the trial solution of the NLS equation for the electric field envelope:

$$\begin{aligned} &A(z,x,y,\tau)\\ =&A_0(z,\tau)\mathrm{e}^{-(x^2+y^2)/r^2(z,\tau)}\mathrm{e}^{\mathrm{i}b(z,\tau)(x^2+y^2)+\mathrm{i}\phi(z,\tau)}, \end{aligned} \tag{8}$$

where A_0, r, b, and ϕ are variational parameters and depend on both z and τ. We only consider the loss of multiphoton absorption, other losses such as the plasma absorption and the loss of collision are neglected. So the dependence of the spot size of beam r on the distance of propagation z can be deduced from Eqs.(4), (7) and (8) by the method introduced in Ref.[8]:

$$\frac{\partial r}{\partial z} = 2br + \gamma k\frac{2^K P_{\mathrm{cr}}^{K-1}}{K\pi^{K-1}r_0^{2K-4}}\frac{P^{K-1}}{r^{2K-3}}\left(1-\frac{1}{K}\right), \tag{9}$$

$$\frac{\partial P}{\partial z} = -\gamma k\frac{2^{K-1}P_{\mathrm{cr}}^{K-1}}{K\pi^{K-1}r_0^{2K-4}}\frac{P^K}{r^{2K-2}}, \tag{10}$$

$$\begin{aligned} \frac{\partial b}{\partial z} =&\frac{2}{r^4} - 2b^2 - \frac{2P}{r^4}\\ &+\left[\frac{4k\alpha K 2^K P_{\mathrm{cr}}^K}{\pi^K(K-1)(2K-2)r_0^{2K-2}}\right]\frac{P^K}{r^{2K+2}}, \end{aligned} \tag{11}$$

where r_0 is defined as the beam radius at $1/e^2$ of the irradiance. $\tau_0 = \tau_{\mathrm{FWHM}}/\sqrt{2\ln 2}$, $r/r_0 \to r$, $br_0 \to b$, $\tau/\tau_0 \to \tau$, and $P/P_{\mathrm{cr}} \to P, z$ is unit of kr_0^2, input power $P = \int |A|^2\,\mathrm{d}x\mathrm{d}y = A_0^2r^2\pi/2$, $P_{\mathrm{cr}} = \lambda_0^2/(2\pi n_0 n_2)$, and $\alpha = kn_e/(2n_c)$. Using the method of Runge–Kutta we can solve equations (9)–(11) numerically.

3. Results and discussion

In our experiment, the laser beam was sent into a 50m-long hallway by two transport mirrors and propagated freely in the air.

Figure 1 illustrates the spark result of simulation with the convergence of the short focal length lens (f=20cm). The energy of the laser pulse is 0.7mJ ($\sim 7P_{\mathrm{cr}}$). When the input power of laser is less than the critical power P_{cr}, the propagation of the laser pulse obeys the law of geometric optics. Due to the self-focusing of the laser beam, the nonlinear focus is at 19.54cm from the origin plane $z = 0$ to the nonlinear focal region. It is in good agreement with the experimental result, about 4mm.

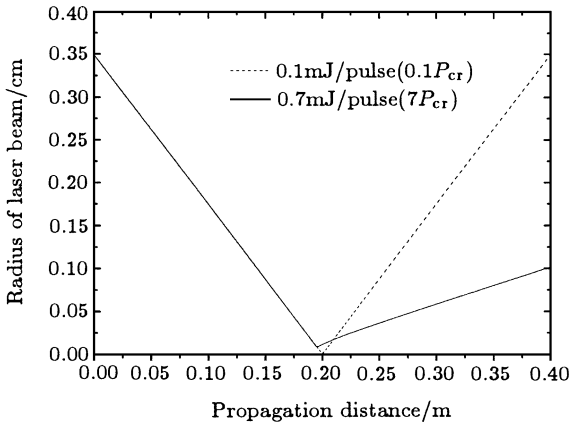


Fig.1. Results of simulation with the convergence of the short focus lens (f=20cm).

With increasing focal length of the lens, the length of the nonlinear focus region increases, but the brightness of the spark weakens. There are different colours in the nonlinear focus, the central part of the spark is bright white light, and the both sides of the spark are of the colours ranging from red to blue. Behind the nonlinear focal region, a violet light appears due to the interaction of the femtosecond laser pulses and the double-molecule of the air. The violet light is the third harmonic wave of the femtosecond laser pulses. It lies at the centre of the laser spot, and its diameter is about one-sixth that of the laser beam. Its profile is different from the profile of the laser beam. We find that this kind of difference is related to the distribution of the intense region of the laser profile. There are yellow and green light regions at the edge of the laser spot, which originate from the spatiotem-

poral self-phase modulation of the laser pulse in the plasma generated by the moving focus.[5] The diameter of the light spot at the nonlinear region is about 160μm. Using photographic papers (Kodak linograph direct print paper) to record the diameter of the filaments, we find that the result of simulation is the same as the experimental measurement.

Figure 2 displays the numerical simulation results for different energies of laser pulse. The laser beam converged with the lens (f=14m) produces an over 10m-long filament. The numerical simulation is basically the same as that measured in the experiments. It can be explained by the modulational instability of femtosecond laser pulses propagating in the air. Figure 3 shows the results of both the experiment measurement and numerical simulation. It shows that the experimental and simulation results are in good agreement with each other. It is well known that the filament process is accompanied by the generation of the supercontinuum white light (Fig.4). We use a camera to record the picture of the supercontinuum white light in order to approve the filament in the process of intense laser pulse propagating in the air.

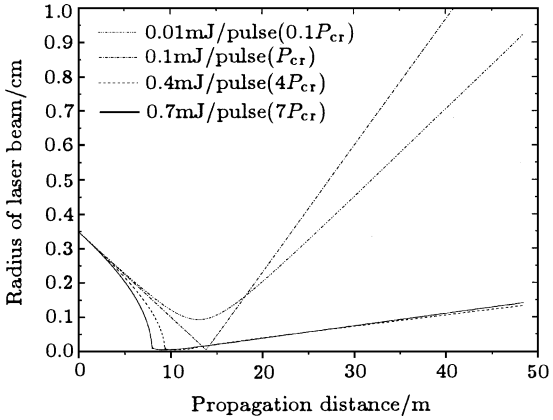


Fig.2. Results of simulation for different energies of laser pulse (f=1400cm).

We use two wedges to the reflect laser beam at a 45° angle. The reflected laser beam is imaged with a large aperture lens and recorded by a CCD camera. The distribution of laser intensity is analysed with the software of the Laser Beam Analyser to obtain the diameter of the laser beam ($1/e^2$ level of intensity). We have observed that two filaments appear at the position of about 8m from the origin plane $z = 0$. They merge into a single filament near the focus of the lens. This occurs from the energy loss of laser pulses due to multiphoton ionization. We found either two filaments or a single filament is always accompanied by the third harmonic generation. The location of the filament varies for different laser pulses. We also observed that the edge of the laser spot does not appear as yellow and green light. This results from the low power of laser pulse.

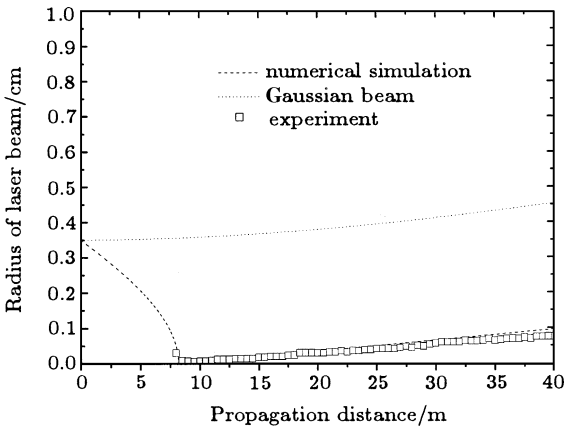


Fig.3. Evolution of the beam radius as a function of propagation distance. The solid squares denote the experimental results. The solid curve is the simulation result using the variational method to solve the NLS equation. The radius of an ideal Gaussian beam, 0.35cm, is plotted (dotted curve) as reference.

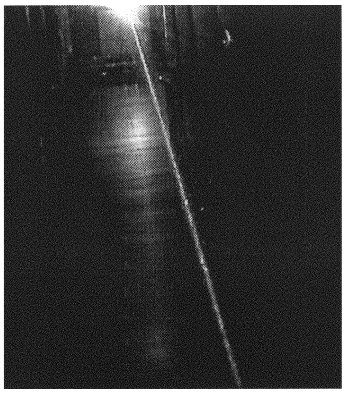


Fig.4. The filament process accompanied by the generation of supercontinuum white light (f=1400cm).

4. Conclusion

We have observed a filament with a length over 10-m generated by femtosecond laser pulses propagating in air with pulse energy of only 0.7mJ and the evolution of the filament (from two filaments to a filament). We found that the higher the incident laser power is, the easier the multifilament is formed, due to the modulational instability of femtosecond laser pulses propagating in the air.

References

[1] La Fontaine B *et al* 1999 *Phys. Plasma.* **6** 1615
[2] Braun A *et al* 1995 *Opt. Lett.* **20** 73
[3] Yang H *et al* 2001 *Phys. Rev.* E **65** 016406
[4] Nibbering E T J *et al* 1996 *Opt. Lett.* **21** 62
[5] Kosareva O G *et al* 1997 *Opt. Lett.* **22** 1332
[6] Sprangle P *et al* 1996 *Phys. Rev.* E **54** 4211
[7] Tzortzakis S *et al* 2001 *Phys. Rev. Lett.* **86** 5470
[8] Couairon A and Bergé L 2002 *Phys. Rev. Lett.* **88** 135003
[9] Aköbek N *et al* 2002 *Phys. Rev. Lett.* **89** 143901
[10] Schillinger H and Sauerbrey R 1999 *Appl. Phys. B: Lasers Opt.* **68** 753
[11] Zhao X M *et al* 1995 *IEEE J. Quantum Electron.* **31** 599
[12] La Fontaine B *et al* 2000 *J. Appl. Phys.* **88** 610
[13] Pépin H *et al* 2001 *Phys. Plasma.* **8** 2532
[14] Chin S L *et al* 1991 *J. Nonlinear Opt. Phys. Mater.* **8** 121
[15] Aköbek N *et al* 2001 *Opt. Commun.* **191** 353
[16] Tzortzakis S *et al* 2001 *Phys. Rev. Lett.* **86** 5470
[17] Talebpour A *et al* 1999 *Opt. Commun.* **163** 29
[18] Aköbek N *et al* 2000 *Phys. Rev.* E **61** 4540
[19] Cerda S Cháez *et al* 1998 *Eur. Phys. J.* D **1** 313